

Soft Sensors and Artificial Neural Networks



Sensors & Transducers

Volume 72
Issue 10
October 2006

www.sensorsportal.com

ISSN 1726-5479

General Editor: professor Nikolay V. Kirianaki, phone: +380 322 762971, e-mail: ifsa@sensorsportal.com

Editor-in-Chief: professor Sergey Y. Yurish, phone: +34 696067716, e-mail: editor@sensorsportal.com

Editorial Advisory Board

- Ahn, Jae-Pyoung**, Korea Institute of Science and Technology, Korea
Arndt, Michael, Robert Bosch GmbH, Germany
Atghiaee, Ahmad, University of Tehran, Iran
Augutis, Vyantas, Kaunas University of Technology, Lithuania
Avachit, Patil Lalchand, North Maharashtra University, India
Bahreyni, Behraad, University of Manitoba, Canada
Barford, Lee, Agilent Laboratories, USA
Barlingay, Ravindra, Priyadarshini College of Engineering and Architecture, India
Basu, Sukumar, Jadavpur University, India
Beck, Stephen, University of Sheffield, UK
Ben Bouzid, Sihem, Institut National de Recherche Scientifique, Tunisia
Bodas, Dhananjay, IMTEK, Germany
Bousbia-Salah, Mounir, University of Annaba, Algeria
Brudzewski, Kazimierz, Warsaw University of Technology, Poland
Cerda Belmonte, Judith, Imperial College London, UK
Chakrabarty, Chandan Kumar, Universiti Tenaga Nasional, Malaysia
Chen, Rongshun, National Tsing Hua University, Taiwan
Chiriac, Horia, National Institute of Research and Development, Romania
Chung, Wen-Yaw, Chung Yuan Christian University, Taiwan
Cortes, Camilo A., Universidad de La Salle, Colombia
Costa-Felix, Rodrigo, Inmetro, Brazil
Cusano, Andrea, University of Sannio, Italy
D'Amico, Arnaldo, Università di Tor Vergata, Italy
Dickert, Franz L., Vienna University, Austria
Dieguez, Angel, University of Barcelona, Spain
Ding Jian, Ning, Jiangsu University, China
Donato, Nicola, University of Messina, Italy
Donato, Patricio, Universidad de Mar del Plata, Argentina
Dong, Feng, Tianjin University, China
Drljaca, Predrag, Intersema Sensoric SA, Switzerland
Erdem, Gursan K. Arzum, Ege University, Turkey
Erkmen, Aydan M., Middle East Technical University, Turkey
Estrada, Horacio, University of North Carolina, USA
Fericean, Sorin, Balluff GmbH, Germany
Gaura, Elena, Coventry University, UK
Gole, James, Georgia Institute of Technology, USA
Gonzalez de la Ros, Juan Jose, University of Cadiz, Spain
Guan, Shan, Eastman Kodak, USA
Gupta, Narendra Kumar, Napier University, UK
Hernandez, Wilmar, Universidad Politecnica de Madrid, Spain
Homentcovschi, Dorel, SUNY Binghamton, USA
Hsiai, Tzung (John), University of Southern California, USA
Jaffrezic-Renault, Nicole, Ecole Centrale de Lyon, France
Jaime Calvo-Galleg, Jaime, Universidad de Salamanca, Spain
James, Daniel, Griffith University, Australia
Janting, Jakob, DELTA Danish Electronics, Denmark
Jiang, Liudi, University of Southampton, UK
Jiao, Zheng, Shanghai University, China
John, Joachim, IMEC, Belgium
Kalach, Andrew, Voronezh Institute of Ministry of Interior, Russia
Katake, Anup, Texas A&M University, USA
Lacnjevac, Caslav, University of Belgrade, Serbia
Li, Genxi, Nanjing University, China
Lin, Hermann, National Kaohsiung University, Taiwan
Lin, Paul, Cleveland State University, USA
Liu, Cheng-Hsien, National Tsing Hua University, Taiwan
Liu, Songqin, Southeast University, China
Lorenzo, Maria Encarnacio, Universidad Autonoma de Madrid, Spain
Matay, Ladislav, Slovak Academy of Sciences, Slovakia
Mekid, Samir, University of Manchester, UK
Mi, Bin, Boston Scientific Corporation, USA
Moghavvemi, Mahmoud, University of Malaya, Malaysia
Mohammadi, Mohammad-Reza, University of Cambridge, UK
Mukhopadhyay, Subhas, Massey University, New Zealand
Neelamegam, Periasamy, Sastra Deemed University, India
Pushkova, Milka, Bulgarian Academy of Sciences, Bulgaria
Oberhammer, Joachim, Royal Institute of Technology, Sweden
Ohyama, Shinji, Tokyo Institute of Technology, Japan
Pereira, Jose Miguel, Instituto Politecnico de Seteabal, Portugal
Petsev, Dimiter, University of New Mexico, USA
Pogacnik, Lea, University of Ljubljana, Slovenia
Prateepasen, Asa, Kingmoungut's University of Technology, Thailand
Pullini, Daniele, Centro Ricerche FIAT, Italy
Pumera, Martin, National Institute for Materials Science, Japan
Rajanna, K., Indian Institute of Science, India
Reig, Candid, University of Valencia, Spain
Robert, Michel, University Henri Poincare, France
Rodriguez, Angel, Universidad Politecnica de Cataluna, Spain
Rothberg, Steve, Loughborough University, UK
Royo, Santiago, Universitat Politecnica de Catalunya, Spain
Sadana, Ajit, University of Mississippi, USA
Sapozhnikova, Ksenia, D.I.Mendeleyev Institute for Metrology, Russia
Saxena, Vibha, Bhabha Atomic Research Centre, Mumbai, India
Shearwood, Christopher, Nanyang Technological University, Singapore
Shin, Kyuho, Samsung Advanced Institute of Technology, Korea
Shmaliy, Yuriy, Kharkiv National University of Radio Electronics, Ukraine
Silva Girao, Pedro, Technical University of Lisbon Portugal
Slomovitz, Daniel, UTE, Uruguay
Stefan-van Staden, Raluca-Ioana, University of Pretoria, South Africa
Sysoev, Victor, Saratov State Technical University, Russia
Thumbavanam Pad, Kartik, Carnegie Mellon University, USA
Tsiantos, Vassilios, Technological Educational Institute of Kaval, Greece
Twomey, Karen, University College Cork, Ireland
Vaseashta, Ashok, Marshall University, USA
Vigna, Benedetto, STMicroelectronics, Italy
Vrba, Radimir, Brno University of Technology, Czech Republic
Wandelt, Barbara, Technical University of Lodz, Poland
Wang, Liang, Advanced Micro Devices, USA
Wang, Wei-Chih, University of Washington, USA
Woods, R. Clive, Louisiana State University, USA
Xu, Tao, University of California, Irvine, USA
Yang, Dongfang, National Research Council, Canada
Ymeti, Aurel, University of Twente, Netherland
Zeni, Luigi, Second University of Naples, Italy
Zhou, Zhi-Gang, Tsinghua University, China
Zourob, Mohammed, University of Cambridge, UK



Optimized Design of Microresonators Using Genetic Algorithm

G.Uma¹, A. Girija², M. Umapathy³

^{1,2,3}Department of Instrumentation and Control Engineering,
National Institute of Technology, Tiruchirappalli, India-620015

¹E-mail: guma@nitt.edu

³E-mail: umapathy@nitt.edu

Received: 4 July 2006 /Accepted: 18 October 2006 /Published: 23 October 2006

Abstract: This paper represents the optimization of micro resonator design using Genetic Algorithm. Optimized physical layout parameters are generated using genetic algorithm. Optimization evaluates parameter by minimizing active device area, electrostatic drive voltage or a weighted combination of area and drive voltage or by maximizing displacement at resonance. Desired resonant frequency and mode frequency separations are governed by the objective function. Layouts are generated for optimized design parameters using Coventorware. Modal analysis is performed and it is compared with the designed resonant frequency.

Keywords: Microresonators; Genetic Algorithm; Resonant frequency

1. Introduction

Micro-Electro-Mechanical Systems (MEMS) are commonly defined as sensor and actuator systems that are made using integrated-circuit fabrication processes. The main advantage of MEMS-based systems when compared with conventional electromechanical systems is the miniaturization and integration of multiple sensors, actuators, and electronics at a low cost. MEMS design usually begins with high-level specifications that describe the desired behavior of devices [1]. Both the physical

configuration and geometries must be chosen such that the resulting device satisfies the design objectives and operating constraints. In general, there are a number of design variables and complex trade-offs between different performance specifications. Therefore, it is difficult to design MEMS by hand.

The designer has two analysis choices: numerical simulation (e.g., finite-element analysis), and behavioral simulation. Numerical simulation involves self-consistent mechanical finite-element analysis coupled with electrostatic boundary element analysis. This requires much iteration by the designer with different values assigned to the device dimensions or other design variables in each iteration. The design procedure is, therefore, time consuming [2]. Also FEA cannot evaluate all the performance metrics of interest, or may be restricted to certain specific domains (like only mechanical analyses or only electrostatic analyses). Behavioral simulation can be accomplished using many different commercial tools, such as SPICE, MATLAB [3] and Saber [4]. Unfortunately, the construction of behavioral models for MEMS components is completely manual, requiring specific device expertise, which is often lacking in a system designer. No rapid design process is available today for MEMS. As a result, fabrication replaces simulation in the iterative loop. This is very expensive, since fabricated prototypes often do not meet performance specifications and, sometimes, are not even functional. Full verification of designs requires months of effort. Therefore the structured design of MEMS devices is essential. In this work structured design of MEMS device using genetic algorithm is presented.

Genetic algorithms are robust and efficient function optimizers, searching for the extremum of a given objective function [5]. Complex functions that often arise in the design work are highly non-linear, multimodal and nondifferentiable. Genetic algorithms allow us to search the design space in which the "best design" resides but whose form is not obvious or intuitive. The genetic algorithm search process is more efficient than trial-and-error methods, and has also been shown to outperform other search techniques such as gradient-based methods. As an example optimized design of microresonator using genetic algorithm is considered in this work. The optimized design variable values are validated using Coventorware.

2. Modeling of Micro Resonators

The microresonator shown in Figure 1 is used to describe design approach to MEMS component design. The specific resonator topology was first described and analyzed by Tang [6]. It is used in resonator oscillators, in filters [7], and as a mechanical characterization test structure to measure Young's modulus of thin films. The central shuttle mass suspended by two folded-beam flexures forms a mechanical mass-spring-damper system. The folded flexure is a popular design choice for the suspension because it is insensitive to buckling arising from residual stress in the polysilicon film. Instead of buckling, the beams expand outward to relieve the stress in the film.

The resonator can be fabricated by a surface-micromachining process MUMPS. The resonator is driven in the preferred (x) direction by electrostatic actuators that are symmetrically placed on the sides of the shuttle. Each actuator, commonly called a 'comb drive,' is made from a set of interdigitated comb fingers. When a voltage is applied across the comb fingers, an electrostatic force is generated which makes the structure to vibrate. The suspension is designed to be compliant in the x direction of motion and to be stiff in the orthogonal direction (y) to keep the comb fingers aligned.

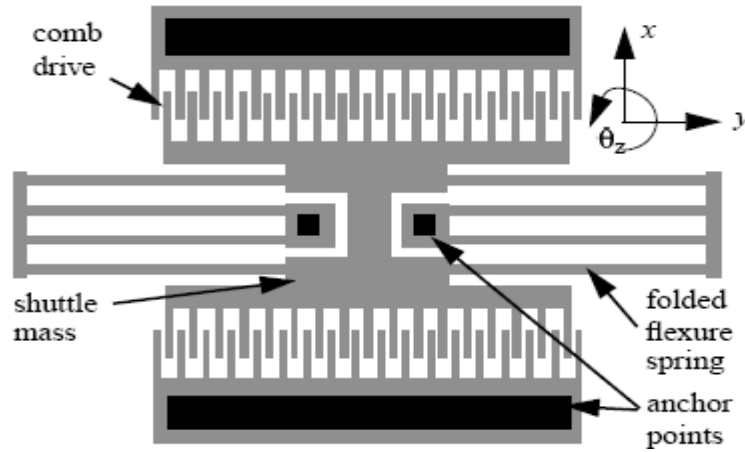


Fig. 1. Folded flexure comb drive resonator.

2.1 Modeling of the oscillation modes

In order to evaluate the performance of a design the models for the device behavior is needed. The preferred direction of motion of the micro resonator is the x-direction. However, the micro resonator structure can vibrate in other modes. Three translation modes along x, y and z and flexure modes are considered for modeling. Effective mass for each mode of interest is calculated by normalizing the total maximum kinetic energy of the spring by the maximum shuttle velocity, v_{max}

$$m_{eff} = \sum_{beam\ i=1}^N \frac{m_i}{L_i} \int_0^{L_i} \left(\frac{v_i(\xi)}{v_{max}} \right)^2 d\xi$$

where m_i and L_i are the mass and length of the i'th beam in the flexure. Analytic expressions for velocities, v_i , along the flexure's beams are approximated from static deformation shapes, and are found from the spring constant derivations.

The net effective mass of the micro resonator in the x-direction (m_x) can be written as

$$m_x = m_{shuttle} + m_{t,eff} + m_{b,eff}$$

where $m_{shuttle}$ is the shuttle mass, $m_{t,eff}$ is the effective mass of all truss sections, $m_{b,eff}$ is the total effective mass of all the beams.

The spring constant in the x direction is given by

$$k_x = \frac{2Et_w^3}{L_b^3} \frac{L_t^2 + 14\alpha L_t L_b + 36\alpha^2 L_b^2}{4L_t^2 + 41\alpha L_t L_b + 36\alpha^2 L_b^2},$$

where E is the Young's modulus of polysilicon, t is the polysilicon thickness, and

$$\alpha = \left(\frac{w_t}{wb} \right)^3.$$

Similarly the modeling equations for y, z and flexure modes can be derived and these are given in the technical report [2]. The total damping force in the x-direction is mainly composed of the forces due to Couette flow below the resonator, Stokes flow above the resonator, and airflow in the gap between comb fingers. The expression for the damping coefficient [8] is

$$B_x = \mu \left[(A_s + 0.5A_t + 0.5A_b) \left(\frac{1}{d} + \frac{1}{\delta} \right) + \frac{A_c}{g} \right]$$

where μ is the viscosity of air ($1.8 \times 10^{-5} \text{Ns/m}^2$), d is the fixed spacer gap between the ground plane and the bottom surface of the comb fingers, δ is the penetration depth of airflow above the structure, g is the gap between comb fingers, and A_s, A_t, A_b and A_c are layout areas for the shuttle, truss beams, flexure beams and comb finger sidewalls, respectively.

General analytic equations for the lateral comb drive force, F_x , as a function of comb finger width w_c , air gap between comb fingers g , structure thickness t , and sacrificial spacer thickness d , are derived in [9]. For the special case of equal comb finger width, gap, thickness, and spacing above the substrate ($w_c = g = t = d$), each comb drive generates a force that is proportional to the square of the voltage, V , applied across the comb fingers.

$$F_x \cong 1.12 \varepsilon_0 N \frac{t}{g} V^2$$

where ε_0 is the permittivity of air, N is the number of fingers in the movable comb drive, V is the instantaneous voltage across the comb fingers. If the comb fingers are not perfectly centered, a y-directed electrostatic force is also present. In the absence of restraining springs, this force will result in snapping of the movable comb fingers and the stationary comb fingers. Assuming a small perturbation δy in the y direction, the destabilizing force, $F_{e,y}$ is proportional to displacement such that $F_{e,y} = K_{e,y} \delta y$, where $k_{e,y}$ is an electrical negative spring constant.

$$k_{e,y} = 2\varepsilon_0 N V^2 x_0 \frac{t}{g^3}$$

If there is a small rotation $\delta\theta$, about the z-axis, a destabilizing electrostatic torque, $\tau_{e,\theta} = k_{e,\theta} \delta\theta$ is generated by the comb drive. The rotational spring constant is found by realizing that the destabilizing force acts through a moment arm, X_c , on the center of the resonator, giving

$$k_{e,\theta} = k_{e,y} X_c^2 \cong 2\varepsilon_0 N V^2 x_0 \frac{t}{g^3} X_c^2,$$

where $X_c = 0.5L_{sa} + w_{cy} + L_c - 0.5x_0$.

3. Optimization Problem Formulation

Formulation of optimization problem involves determining the design variables, the numerical design constraints, and the quantitative design objective. The synthesis is achieved through an optimization algorithm, which seeks to minimize a cost function and simultaneously satisfy the constraints. Fifteen design variables are identified for the proposed micro resonator structure. The design variables are listed in Table 1 and shown in Figure 2. These include 13 geometrical parameters, the number of fingers in the comb drive N , and the effective voltage V . The voltage V equals $\sqrt{2V_{ac}V_{dc}}$ where V_{dc} represents dc voltage applied to the shuttle, and V_{ac} , indicates the sinusoidal voltage applied to one side of comb drive actuator. Technology driven design rules set minimum widths and minimum spaces between structures. Maximum beam lengths are constrained to $400\mu\text{m}$ to avoid problems with undesirable curling due to stress gradient in the structural film and possible sticking and breakage during the wet release etch. Maximum width of beams is constrained to $20\mu\text{m}$ by the limited undercut of PSG to release the structures. The shuttle axle, the shuttle yoke and the comb yoke are at least $10\mu\text{m}$ wide so that, they are relatively more rigid than folded – flexure beams.

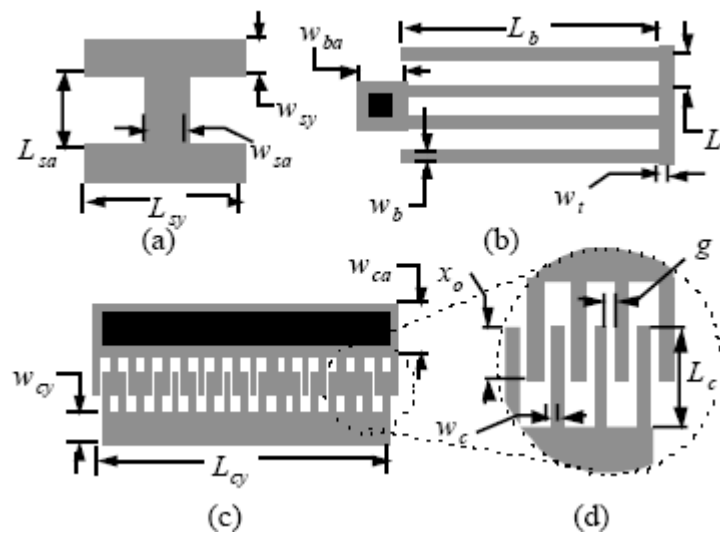


Fig. 2. Dimensions of the micro resonator elements: (a) shuttle mass, (b) folded flexure, (c) comb drive with N movable ‘rotor’ fingers, (d) close up views of comb fingers.

3.1 Geometric and functional constraints

The constraints can be classified into two kinds: geometrical constraints, which are directly related to the physical dimensions of the micro resonator and functional constraints, which are related to the behavior of the micro resonator. The constraints are detailed in Table 2. The resonator width and length must not exceed an arbitrary fixed size, set at $700\mu\text{m}$.

Table 1. Design Variables.

Design variables			
Variables	Description	Min	Max
L	Length of flexure beam	2	400
W_b	Width of flexure beam	2	20
L_t	Length of truss beam	2	400
W_t	Width of truss beam	2	20
L_{sy}	Length of shuttle yoke	2	400
W_{sy}	Width of shuttle yoke	10	400
W_{sa}	Width of Shuttle axle	10	400
W_{cy}	Width of comb yoke	10	400
L_{cy}	Length of comb yoke	2	700
L_c	Length of comb fingers	8	400
W_c	Width of comb fingers	2	20
g	Gap between comb fingers	2	20
x_0	Comb finger overlap	4	400
N	Number of comb fingers	1	100
V	Voltage amplitude	1	50
STYLE VARIABLES			
W_{ba}	Width of beam anchors	11	11
W_{ca}	Width of stator comb anchors	14	14

Table 2. Geometric Constant.

Constraint Description	Expression	Min [μm]	Max [μm]
Actuator length	$L_{cy} + 2g + 2w_c$	0	700
Comb- fill	$(2N + 1)w_c + 2Ng$	L_{cy}	L_{cy}
Flexure length	$L_{sy} + 2L_b + 2w_t$	0	700
Total resonator width	$3L_t + w_{sy} + 4L_c - 2x_0 + 2w_{cy} + 2w_{ca}$	0	700
Comb clearance during motion	$L_c - (x_0 + x_{disp})$	4	200
Minimum comb overlap	$x_0 - x_{disp}$	4	200
Shuttle clearance during motion	$L_t - x_{disp} - (w_{sy} + w_b) / 2$	4	200
Shuttle gap in y	$(L_{sy} - 2w_{ba} - w_{sa}) / 2$	2	200

The functional design constraints are listed in Table 3. The resonant frequency constraint ensures that the user specification on frequency (f_{spec}) is met. The next two constraints ensure that the resonator moves adequately at resonance and has a quality factor greater than 5, respectively. The mode decoupling constraints are necessary to ensure that the x-mode resonant frequency dominates. The three in-plane resonant frequencies f_i are constrained to be at least thrice that of the x-mode while the out-of-plane resonant frequencies (f_o) are constrained to be at least twice that of the x-mode. For stability, the restoring force of the spring in the y direction must be three times greater than the destabilizing electrostatic force from the comb drive (i.e., $3k_{e,y} < k_y$). A similar stability constraint must hold for the rotational mode.

Table 3. Functional constraints.

Constraint Description	Expression	Min	Max
Resonant frequency	f_x / f_{spec}	0.98	1.02
Stroke at resonance	x_{disp}	2 μm	100 μm
Quality factor in x	Q_x	5	10^5
y-axis stability	$k_{e,y} / k_y$	0	1/3
θ_z stability	$k_{e,\theta z} / \theta_z$	0	1/3
In-plane mode separation	f_x / f_i	0	1/3
Out-of-plane separation	f_x / f_o	0	1/2
k_x accuracy	x_{disp} / L_b	0	1/10

4. Optimization Using Genetic Algorithm

Three objective functions are chosen to minimize: total resonator active area, amplitude of the comb-drive voltage, and the sum of active area and drive voltage, and the sum of active area and drive voltage normalized to the maximum possible area and voltage; and a fourth objective function to maximize: displacement at resonance.

The general non-linear constrained optimization formulation can be written as

$$\min_{u,x} \sum_{i=1}^k w_i f_i(u, x)$$

$$\min_{u,x} f(u, x),$$

such that

$$h(u, x) = 0$$

$$g(u, x) \leq 0$$

$$u \in U_p,$$

where u is the vector of design variables given in Table 1; x is the vector of state and style variables; $f(u, x)$ is objective function that codify performance specifications the designer wishes to optimize, e.g., area; and $h(u, x) = 0$ and $g(u, x) \leq 0$ are each a set of functions that implement the geometric and functional constraints given in Tables 2 and 3. The constrained problem is solved by using genetic algorithm. Genetic algorithms are adaptive methods, which may be used to solve search and optimization problems.

Before a genetic algorithm can be run, a suitable encoding (or representation) for the problem must be devised. A fitness function is also required, which assigns a figure of merit to each encoded solution. During the run, parents must be selected for reproduction, and recombined to generate offspring.

It is assumed that a potential solution to a problem may be represented as a set of parameters. These parameters (known as genes) are joined together to form a string of values (chromosome). In genetic terminology, the set of parameters represented by a particular chromosome is referred to as an individual. The fitness of an individual depends on its chromosome and is evaluated by the fitness function.

The individuals, during the reproductive phase, are selected from the population and recombined, produced offspring, which comprise the next generation. Parents are randomly selected from the population using a scheme, which favours fitter individuals. Having selected two parents, their chromosomes are recombined, typically using mechanisms of crossover and mutation. Mutation is usually applied to some individuals, to guarantee population diversity. Figure 3 gives a flow chart for the basic genetic algorithm.

For optimized parameter generation using genetic algorithm, coding is developed using Matlab. The initial population is randomly generated for 16 design variables whose values are bounded within minimum and maximum specification given in Table 1. The geometric (Table 2) and functional (Table 3) constraints are checked with randomly generated chromosome. If all the constraints are satisfied, objective function is evaluated. Roulette wheel selection technique is used to select good string from the initial population. The following parameters are used for GA coding: 15-gene chromosome, population size=20, number of generations =50, Selection scheme=Roulette wheel, mutation probability $p_{\text{mutation}} = 0.05$, Crossover probability $p_{\text{crossover}} = 0.8$.

Resonators are synthesized using all five objective functions ranging from 14 kHz to 300 kHz. From the optimized results, it is clear that parameter synthesis explore a different region of the design space, leading to the diverse layouts based on the selection of objective function. Selected design parameters for the synthesized resonators with maximized displacement are shown in Figure 4. Optimized dimensions of micro resonator for frequency 36 kHz with maximized displacement as objective function is given in Table 4.

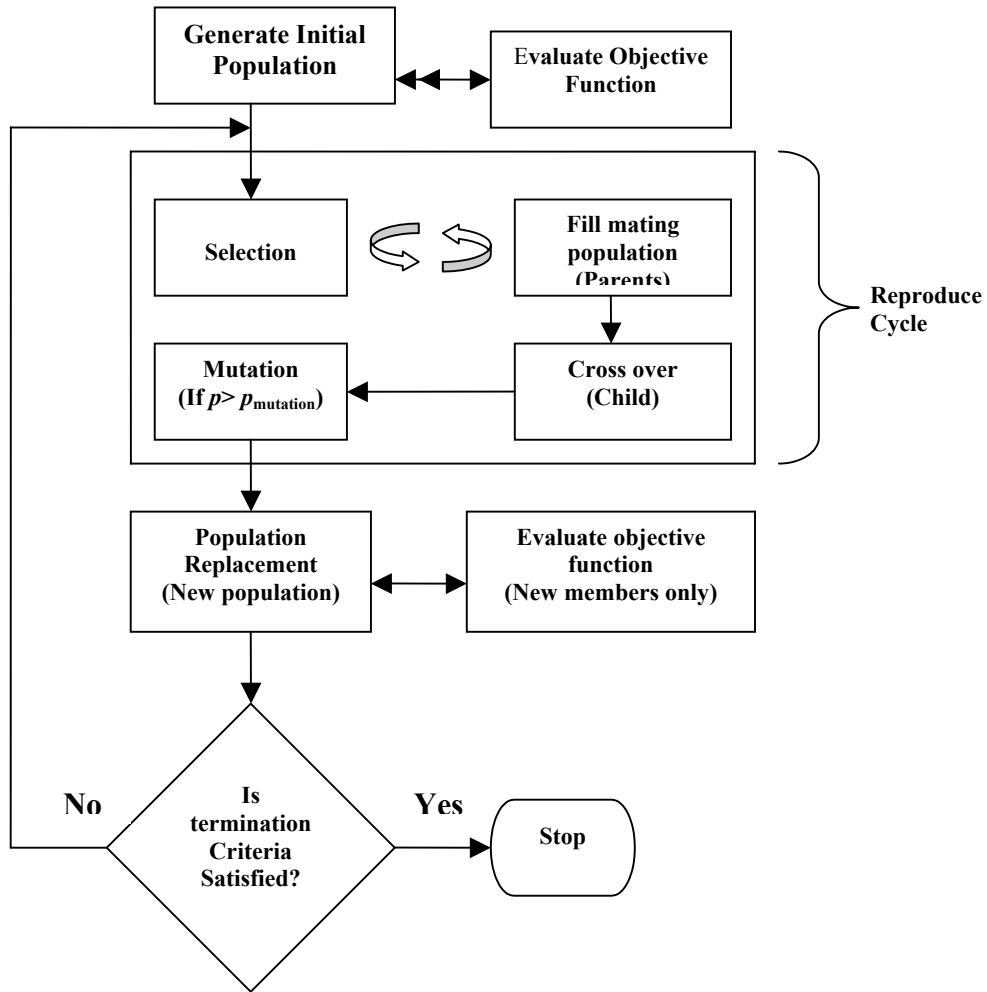


Fig. 3. Basic Genetic Algorithm flowchart.

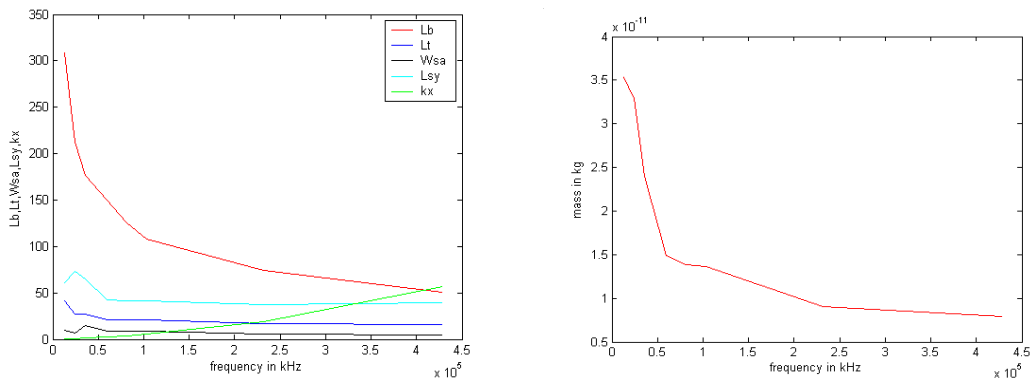


Fig. 4. Selected Parameter values for synthesized resonators with maximized displacement.

Table 4. Optimized dimensions of micro resonator for frequency 36kHz.
All units are in μm except voltage.

Length of flexure beam	176.53	Length of comb yoke	312.25
Width of flexure beam	2.03	Length of comb fingers	88.61
Length of truss beam	28.71	Width of comb fingers	2.5
Width of truss beam	11.01	Gap between comb fingers	2.5
Length of shuttle yoke	65.48	Comb finger overlap	60.85
Width of shuttle yoke	11.61	Number of comb fingers	31
Width of Shuttle axle	14.37	Voltage amplitude	44
Width of comb yoke	13.63		

5. Design Validation Using Coventorware

The synthesis results are evaluated by comparing the predicted behavior to finite element analyses. From optimized results micro resonator layout is created using 2-D layout Editor and 3D model of the same is built by 3-D builder in CoventorWare. The finite element analysis of the designed structure is carried out using MemMECH module by using Manhattan type of meshing with element size of $2\mu\text{m} \times 2\mu\text{m} \times 4\mu\text{m}$, which is found to be optimized mesher setting.

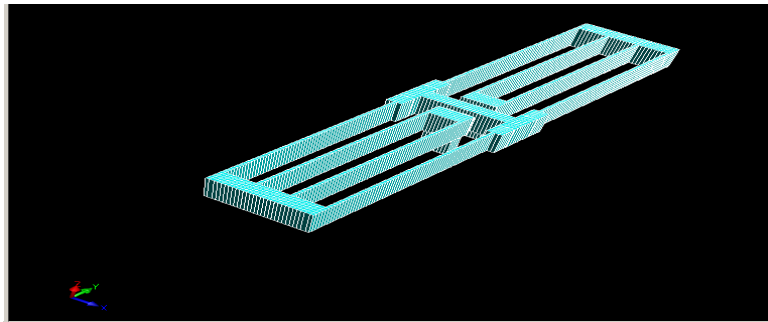


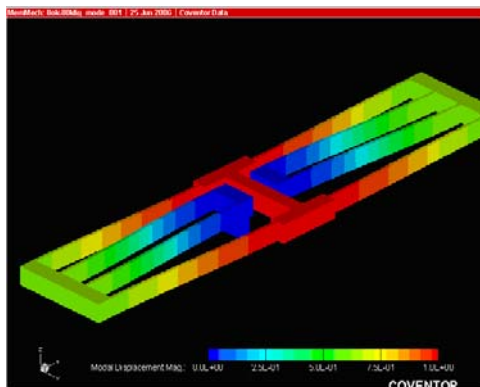
Fig. 5. Meshed model.

The modal analysis is used to find the natural frequency of the structure. Table 5 shows the modal frequencies from MemMech analysis for the layout designed for 79 kHz. The mode shapes represent the overall deformation of the proof mass oscillating at the associated modal frequency. Modal shapes for the first six modes are shown in Figure 6. The first and third mode is the translation mode along x and z-axis respectively. Fourth mode is rotational mode along x-axis and sixth mode is anti flexural mode. The preferred direction of motion of the micro resonator is along x-axis. From modal analysis results, it is clear that the objective is satisfied since it is the first mode.

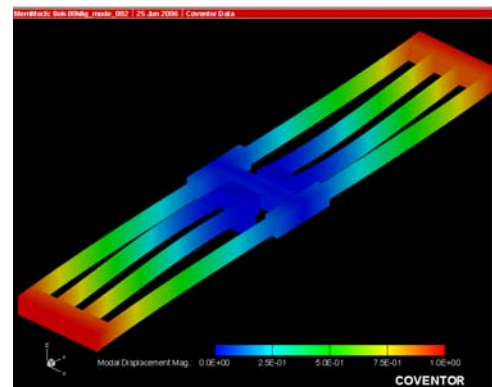
The synthesized microresonators were simulated with Coventorware using 3D beam elements and the frequencies of modes were compared to the frequencies predicted by the analytical models.

Table 5. Modal analysis Results.

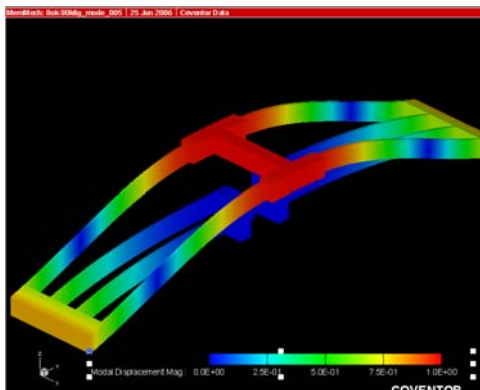
S. No	Frequency	Generalized mass
1	7.4415e04	1.5e-11
2	7.762717e04	9.578e-12
3	7.888452e04	1.5387e-11
4	1.221104e05	7.89978e-12
5	1.359506e05	1.34889e-11
6	1.55624e05	1.164308e-11



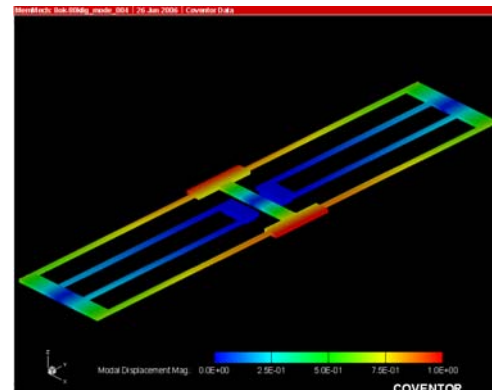
(a)



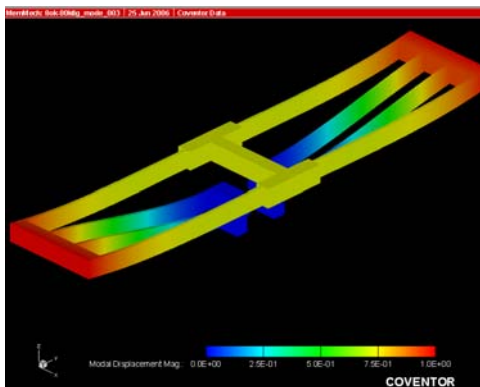
(b)



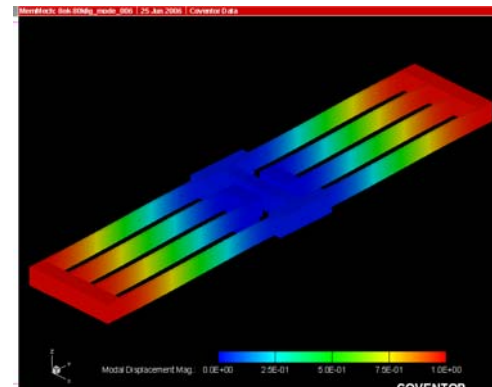
(c)



(d)



(e)



(f)

Fig. 6. Mode shapes (a) mode1 (b) mode 2 (c) mode3 (d) mode 4 (e) mode 5 (f) mode 6.

Comparison of simulated and designed frequency values of x, z and flexure mode is given in Table 6.

Table 6. Desired and simulated frequency values.

fx spec	1.31e04	2.4e04	3.8e04	5.8e04	8e04	1e05	2.2e05	4.2e05
fx sim	1.25e04	2.3e04	3.5e04	5.6e04	7.4e04	9.7e04	2.0e05	3.8e05
fz spec	1.63e04	2.9e04	4.7e04	7.2e04	9.9e04	1.2e05	2.7e05	5e05
fz sim	1.41e04	2.8e04	3.8e04	6.141e04	7.8e04	1.0e05	2.1e05	4.1e05
fflspec	3.39e04	6.9e04	9.8e04	1.48e05	2.0e05	2.5e05	5e05	1e06
fflsim	2.98e04	6.8e04	7.9e04	1.22e05	1.6e05	2.0e05	4.8e05	9.2e05

From the table it is seen that the simulated and specified frequency values from 14kHz to 300kHz are nearly equal. Layouts are synthesized for the above frequency range with minimized area and maximum displacement as objective junction. From Figure 7 and 8 it is observed that the resonators become smaller with increasing values of resonant frequency. Smaller devices have less mass, and smaller flexures are stiffer. Increasing the resonator frequency requires an increase in stiffness, k_x which can be accomplished using shorter beams L_b .

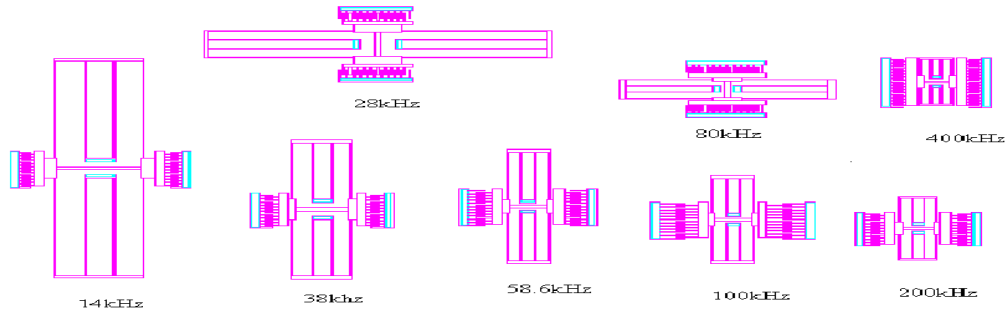


Fig. 7. Layout synthesized using coventorware with minimized area as objective function.

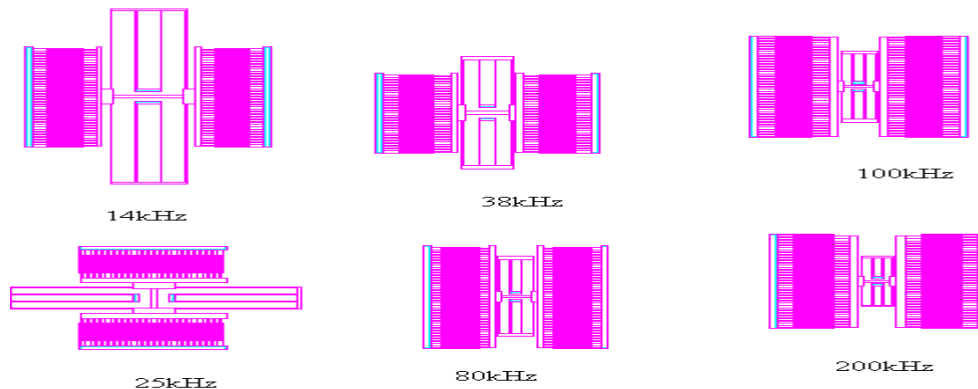


Fig. 8. Layout synthesized with maximum displacement as objective function.

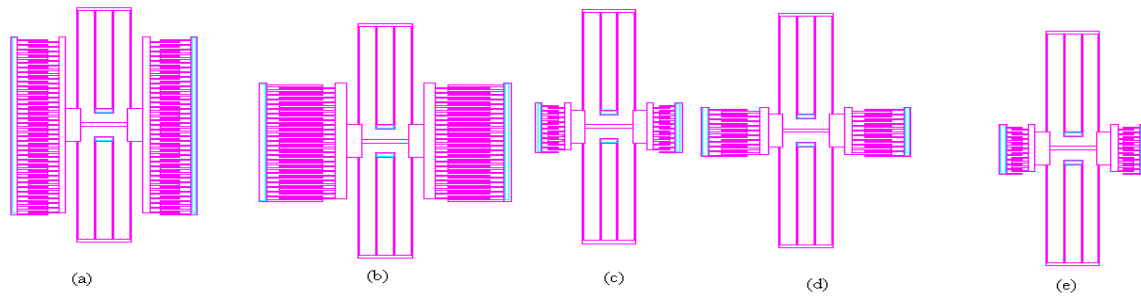


Fig. 9. Comparison of layouts synthesized for 13kHz frequency for different objective function: (a) Minimum voltage; (b) Maximum displacement; (c) Minimum area; (d) Multi objective; (e) Normalized sum of active area and voltage.

Electrostatic actuation with low driving voltage is an important design specification in microresonator design. Driving voltage can be minimized by increasing the number of fingers. For obtaining maximum displacement the length of the finger should be more since the displacement is high. Furthermore, the minimum area resonators tend to have the fewest fingers, sum of area and voltage resonators tend to trade off between fingers and drive voltage. From Figure 9 it is seen that simulated layout for minimum voltage has more fingers, minimum area with fewer fingers and maximum displacement with longest fingers.

Conclusion

Optimal design of folded flexure electrostatic comb drive micro resonator models is successfully done using genetic algorithm. Optimization problem is formulated with all necessary design variables, constraints and for different objective functions. The in-plane and out of plane mode separation constraints ensure that the other modes of vibration are well separated from the x-mode of vibration. The nonlinear constrained optimization problem is solved using genetic algorithm. The genetic algorithm search process is more efficient than traditional methods, and has also been shown to outperform other search techniques such as gradient-based method. Layouts are synthesized for 14 kHz to 300 kHz frequency range in Coventorware using optimum parameter values. MemMech analysis is used to simulate the mechanical behavior of the micro resonators. The specified resonant frequency and simulated resonant frequencies for x, z and flexural modes are compared.

References

- [1]. T. Mukhejee, G.K. Fedder, Structured design of microelectromechanical systems, *Proc. 34th Design Automation Conference (DAC '97)*, Anaheim, CA, June 9-13, 1997.
- [2]. S. Iyer, T. Mukhejee, G.K. Fedder, Optimal synthesis of the folded- flexure comb - drive microresonator, *Technical Report*, Carnegie Mellon University, 1997.
- [3]. G. K. Fedder, Simulation of Microelectromechanical Systems, *Ph.D. Thesis*, Dept. of Electrical Engineering and Computer Science, University of California at Berkeley, Sept. 1994.
- [4]. I. Getreu, Behavioral Modeling of Analog Blocks using the SABER Simulator, *Proc. Microwave Circuits and Systems*, pp 977-980, August 1989.
- [5]. Kalyanmoy Debb, Optimization for Engineering: Design, Algorithm and Examples, Eastern Economy Edition.
- [6]. W.C. Tang, T.C.H. Nguyen, M.W. Judy, R.T. Howe, Electrostatic comb drive of lateral polysilicon resonators, *Sensors and Actuators A 21* (1990) 328-331.

- [7] CT.-C. Nguyen, R.T. Howe, Micromechanical resonators for frequency references and signal processing, *Proc. IEEE Int. Electron Devices Meeting*, San Francisco, CA, 1994, p. 343.
 - [8] X. Zhang and W. C.Tang , Viscous Air damping in driven lateral microresonators, *Sensors and materials*, V.7, No.6, 1995, pp.415-430.
 - [9] W.A. Johnson, L.K. Warne, Electrophysics of micromechanical comb actuators, *J. Microelectromech. Syst.* 4 (1) (1995) 49-59.
-

2006 Copyright ©, International Frequency Sensor Association (IFSA). All rights reserved.
(<http://www.sensorsportal.com>)



UFDC-1

Universal Frequency-to-Digital Converter (UFDC-1)

- 16 measuring modes: frequency, period, its difference and ratio, duty-cycle, duty-off factor, time interval, pulse width and space, phase shift, events counting, rotation speed
- 2 channels
- Programmable accuracy up to 0.001 %
- Wide frequency range: 0.05 Hz ...7.5 MHz (120 MHz with prescaling)
- Non-redundant conversion time
- RS-232, SPI and I²C interfaces
- Operating temperature range -40 °C...+85 °C

www.sensorsportal.com info@sensorsportal.com SWP. Inc.